A New Approach of Image Denoising Based on Adaptive Multi-Resolution Technique

L. M. Satapathy[1], P. Das[2]

[1]Department of Electrical and Electronics Engineering, Siksha 'O'Anusandhan deemed to be University, Bhubaneswar, Odisha, India.
[2]Department of Electrical Engineering, Indira Gandhi Institute of Technology, Sarang, Odisha, India.

ABSTRACT: Medical imaging and diagnostic techniques have become popular over the last two decades with the advancement of data science, data analysis, data storage, and the internet. The impact of this evolution can be seen in the fields of telemedicine and medical sciences, which allow more effective detection and treatment of various diseases. Like any other form of imaging technique, medical images are sensitive to noise and artifacts. The images become unclear with the presence of noise, and the diseases cannot be identified properly. Therefore, image denoising plays a vital role in the field of biomedical image processing. As a result, work must be done to minimize noise without sacrificing image quality. Various methods for reducing noise have already been proposed in the literature. Each method has its own set of benefits and drawbacks. In this paper, we introduce a bi-dimensional empirical mode decomposition (BEMD)-based image de-noising approach. The principal purpose of this research is to decompose noisy images depending on frequency and create a hybrid algorithm that incorporates existing de-noising approaches. The proposed algorithm is an image-dependent technique that decomposes the noisy image into several IMFs with residue, then considering the individual attributes of the IMFs, they are separately filtered. Furthermore equalization is applied to the residue for preserving the edge information. A comprehensive study is conducted over the experimental results of the benchmark test images using different performance measure matrices to quantify the effectiveness of the presented approach. In terms of subjective and objective evaluation, the reconstructed image is found to be more accurate and visually pleasing. It also outperforms the state-of-the-art image-denoising methods, especially in terms of PSNR, RMSE, correlation, and structural similarity.

KEYWORDS: Image de-noising, Adaptive multi-resolution, BEMD, PSNR, RMSE, SSIM.

[Received Aug. 2, 2021; Revised Dec. 20, 2021; Accepted Mar. 15, 2022] Print ISSN: 0189-9546 | Online ISSN: 2437-2110

I. INTRODUCTION

One of the fundamental challenges in the field of medical imaging is the radiation-sensitive property. Due to this property, various noises are encountered during the image acquisition process. The emergence of noise is random in nature and is intimately linked to image quality assessment. In the presence of these undesirable elements, image processing operations are similarly hampered. As denoising plays an important role in the application areas of image processing, such as video tracking, image analysis, restoration, registration, segmentation, and classification, where visually pleasing images are essential, a special focus is required on it (Gonzalez and Woods 2007).

Removing noise from the noisy image is still a challenging problem for researchers. Over the previous few decades, a number of authors have presented many algorithms, each with its own set of benefits and drawbacks. Some of the publications focused on the classification of noises based on their behaviour. The noises discussed in the preceding articles are either additive or multiplicative. Classical filters like as mean filters, median filters, Gaussian filters, and others are employed for spatial domain denoising (Mallat, 2008). But these classical filters not only smooth the image. However, these classical filters not only smooth the image but also blur the edges of the information. In due course, to overcome the above limitations, transformation-based filters were introduced. The Fourier Transform (FT) is one of the transformation and decomposition methods used in image processing. Later on, wavelet transformation became popular as it has a low resolution and provides simultaneous localization in the time and frequency domains.

The Wavelet transform (WT) (Gupta and Ahmad 2018; Ellinas et al. 2004) has shown its efficiency in various signal processing applications. The beauty of this method is that the decomposed signal contains the different space-frequency components. At this stage, many authors have applied some mathematical operation such as thresholding to suppress the noise (Ellinas et al. 2004; Zhang 2016; Fedak and Nakonechnyy 2015; Kimlyk and Umnyashkin 2018). Then the denoised image is reconstructed by reversing the wavelet coefficients into the spatial domain. The whole process is known as the wavelet-based denoising technique (Fedak and Nakonechnyy 2015; Kimlyk and Umnyashkin 2018; Bnou et al. 2020; Sagheer and George 2020). As per image quality, this denoising method gives a better result in terms of PSNR.

*Corresponding author: lalitmohan.satapathy@gmail.com
doi: http://dx.doi.org/10.4314/njtd.v19i1.10

Moreover, in maximum denoising cases, wavelet thresholds are applied to remove the Gaussian noise. Popular thresholding techniques used in wavelets are soft thresholding and hard thresholding (Donoho, 1995; Kumar, 2013). In soft thresholding, over smoothing affects the reconstructed image, whereas, in the case of hard thresholding, many coefficients of wavelet become zero, which causes blur and artifacts. Therefore, even though threshold based image denoising methods present favourable results, the artefacts are still noticeable (Fan, Zhang et al, 2019; Srivastava et al, 2016; Madadi et al, 2013). In addition, the wavelet transform has lower singularity and directional effect issues. From an operational point of view, DWT decomposes an image into a set of mutually orthogonal wavelet basis, for which a constant set of filters are used and these filters are not image dependent. Moreover, the inverse DWT increases the computational complexity (Chang et al, 2000; Adamo et al, 2013).

This motivated us towards an image-dependent decomposition method such as bi-dimensional empirical mode decomposition (BEMD) (Yan et al. 2013). The BEMD method is a time-domain analysis suitably used for the analysis of non-linear and non-stationary signals. By applying EMD, the image is decomposed adaptively into integral oscillatory components, and these separate components are named Intrinsic Mode Functions (IMF). The major challenges considered in this paper are the smoothing of flat areas, the protection of edge information without blurring, the preservation of internal texture, and the new artefact suppression.

To outline the paper's objective, section II demonstrates the detailed methodology in algorithm form. Section III describes the experimental results as well as comparisons with other state-of-art methods with proper evidence. The conclusion and future work are given in section IV.

II. MATERIALS AND METHODS

In this section, some of the fundamental issues related to image denoising with different types of noises having zero mean and finite variance are considered and their characteristics are elaborately discussed.

A. BEMD-based Denoising

1) Noise model

In the spatial domain, noise is broadly categorised as additive or multiplicative. The best additive noise used in maximum research work is Gaussian noise. The additive noise model is represented as:

$$I(x, y) = M(x, y) + n(x, y) \quad (1)$$

where $I(x, y)$ is the noise-contaminated image function, $M(x, y)$ is the original image, and $n(x, y)$ represents the signal-independent additive Gaussian random noise with zero variance (Gonzalez and Woods, 2007).

In some cases, noise arises due to environmental conditions such as voltage spikes in the circuits or random changes in the physical properties of materials. This kind of noise is categorised as multiplicative noise and is also known as "speckle" noise. The multiplicative noise model can be depicted as Eq. (2) (Gonzalez and Woods, 2007).

$$I(t) = (I - e)\, M(t) + n(t) \quad (2)$$

where $0 \leq e \leq 1$, with a probability p, $I(t)$ is the noisy image at a particular time (t), $M(t)$ is the original signal, and $N(t)$ is the speckle noise introduced during image capture, transmission, or other processing.

2) Image decomposition

Image decomposition is an image processing technique where the image is segregated into multiple images based on its features and frequency. In this paper, we have used frequency-based decomposition using BEMD (Yan et al, 2013). The EMD can decompose the image into n levels based on the frequency of the input signal. In this model, we have used a four-level decomposition as illustrated in Figure 1.

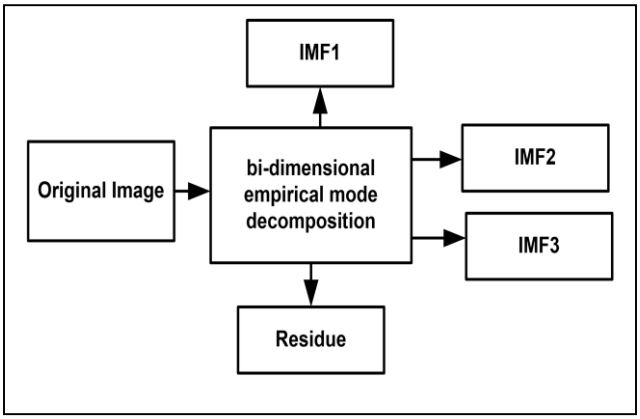

Figure 1: Image decomposition using BEMD.

3) Image denoising model

Figure 2 demonstrates the proposed denoising model. In step 1, the data acquisition system is modelled such that the original signal is corrupted by the external noise. The noisy image (I) is decomposed into four parts using BEMD based on their frequency. Where the decomposed images from high frequency to low frequency are depicted as IMF_1, IMF_2, IMF_3, and residue. The objective of this algorithm is to clean up the noise available in the homogeneous areas and preserve the structures like edges and corners. Owing to this, the conservation of valuable hidden information can be achieved by separately considering the decomposed images (Yan et al, 1998). Noise is often high-frequency in nature and the high-frequency.

Moreover, noise is often high-frequency in nature. Therefore, the high-frequency components of digital images are filtered to suppress the noise. As the low-frequency component holds the details of hidden structures as their pixel values change slowly over space, the residue of the image is made unfiltered. In addition, the residue is equalised to improve the brightness.

B. Bidimensional Empirical Mode Decomposition (BEMD)

The noisy medical image can be decomposed into a finite number of unique frequency components, which are known as intrinsic mode functions (IMF) (Satapathy et al, 2018; Dong et al, 2014). These IMFs are extracted by applying a sifting process that repeats the steps until less than 2 maxima points occur.

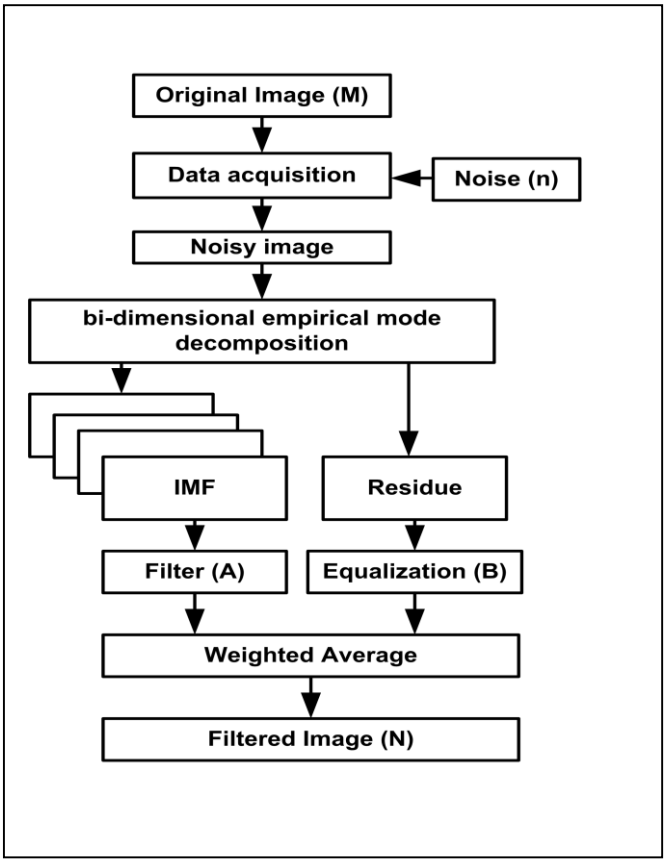

Figure 2: Image denoising using BEMD.

The uniqueness of the BEMD is similar to that of the EMD, which is used for one-dimensional signals. If I (x,y) is defined as the image which is to be decomposed into a series of BIMFs and a residue Eqn.(3).

$$I(x,y) = \sum_{i=1}^{K} IMF_i\,(x,y) + \mathrm{Res}\,(x,y) \qquad (3)$$

where the *IMFi* (*x*, *y*) is the i^{th} IMF component. The frequency of *IMF*1 is higher than the other *IMF*s. The detailed process is demonstrated in Figure 3.

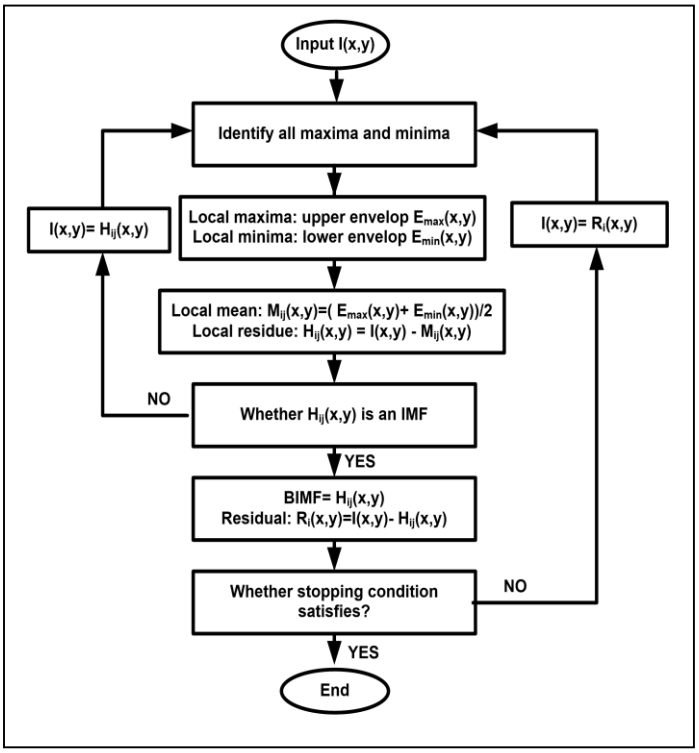

Figure 3: Flowchart of BEMD.

C. Noise

Noise is treated as external energy that corrupts the signal and changes its characteristics. *Salt-and-pepper noise* is also known as impulse noise, which is a form of white and black pixel that can sometimes be seen on images. The probability density function (PDF) "S" of salt and pepper noise with variable "u" is formulated as follows:

$$\begin{aligned} S(u) &= S_P && \text{for } u = 0 \text{ (Pepper)} \\ &= Ss && \text{for } u = 2^n - 1 \text{ (Salt)} \\ &= 1 - (Sp - Ss) && \text{for } u = k\ (0 < k < 2^n - 1) \end{aligned} \qquad (4)$$

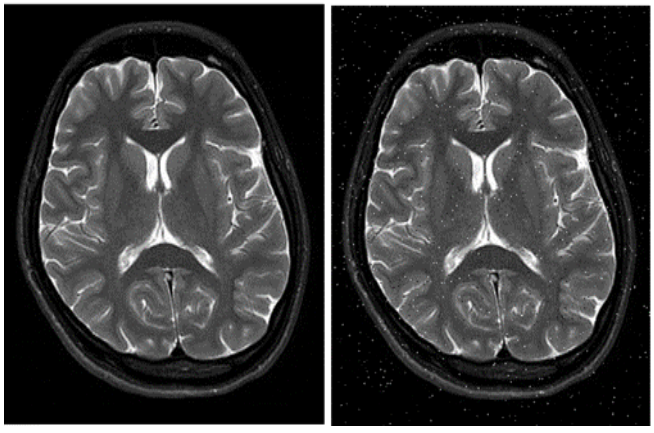

(a) **(b)**

Figure 4: (a) Input MRI brain images (b) Image with salt and pepper noise and 0.01 variance.

C) Gaussian Noise

This is statistical noise that is identically distributed at any two points in time. Sensor noise, which is caused by temperature and poor lighting, is the primary source of Gaussian noise. The probability density function *G* of a Gaussian random variable is given by:

$$G(Z) = \frac{1}{\sigma\sqrt{2\pi}} e^{-\frac{(Z-\mu)^2}{\sigma^2}} \quad (5)$$

where *Z* represents the intensity of pixel the parameters μ *and* σ represent the mean and standard deviation.

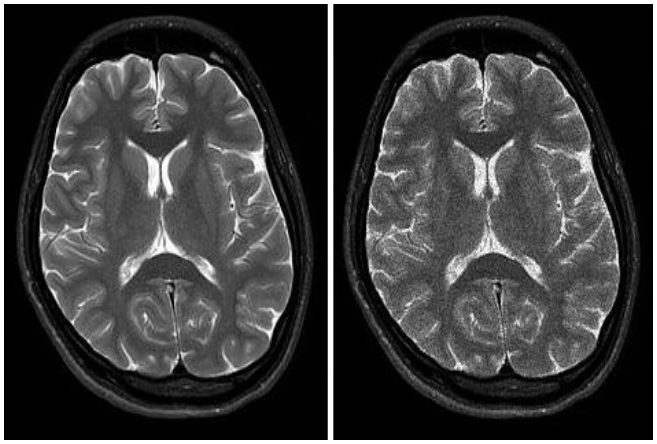

(a) (b)

Figure 5: (a) Input MRI brain images (b) image with Gaussian noise and 0.01 variance.

D) Speckle Noise

This is modelled as a multiplicative noise that arises due to the effect of environmental conditions. The probability density function F of speckle noise follows the gamma distribution and can be represented as follows in Eqn. 6.

$$F(g) = \frac{a^b g^{b-1}}{(b-1)!} e^{-ag} \quad (6)$$

where *g* is the grey level intensity, *a* and *b* are positive integers. The mean and variance of this density are b/a and b/a^2. For an 8-bit imaging system, the a and b lies between 0 and 255.

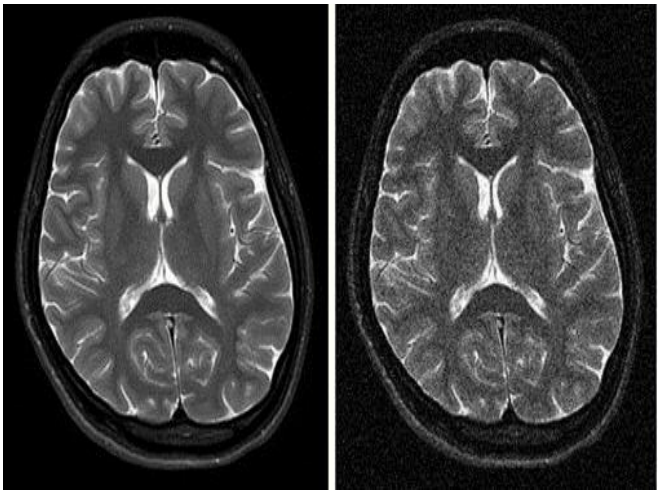

(a) (b)

Figure 6: (a) Input image MRI brain images (b) image with Speckle noise and 0.01 variance.

E) Filters

Nowadays, filters are used for the suppression of high-frequency components of an image. As a result, the image is smoothed and the edge is preserved. Compared with the frequency-domain, in the spatial domain, noise removal is easier because it requires much less processing time. The filters are broadly divided into two categories: (i) linear filters and (ii) non-linear. The linear filter has the advantage of faster processing but fails to preserve the edge where a nonlinear filter can preserve the edge with the compromise of processing speed.

F) Median Filter

This is a non-linear filter having the ability to remove salt and pepper type noise by using a pre-defined window size. During the filtering process, the median filter replaces the pixel values with the median value of neighbouring pixels. Since edge information is important for an image, the median filter is useful for protecting edges during smoothing.

$$M' \leftarrow \text{median}\{M(i+u,j+v) \mid (u,v) \in R\} \quad (7)$$

where M' is the filtered image and $-1 < (u, v) < 1$.

G) Gaussian filtering

This is a linear filter. During the filter process, it usually blurs theedges andreduces the details. The standard deviation used in the Gaussian function is playing a vital role in its behavioral feature.In the digital image domain,a two-dimensional Gaussian function is used.

$$G(p,q) = \frac{1}{2\pi\sigma^2} e^{\frac{p^2+q^2}{2\sigma^2}} \quad (8)$$

where p and q are the horizontal and vertical distances of the pixel from the origin. σ is the standard deviation. A Gaussian filter reduces the contrast and preserves the brightness of the filtered image. As per its characteristics, it is designated as the ideal time-domain filter.

H) Wiener Filter

This is a stationary linear filter used for inverse filtering and noise smoothing. In inverse filtering, the filter works as a high-pass filter by using de-convolution. In compression mode, it functions as a low-pass filter to remove noise and minimise the overall mean square error. This technique gives a better result in the case of additive white Gaussian noise (AWGN). The limitation of Wiener filtering is that it requires knowledge of the power spectra of the noise and the original image. The Wiener filter can be mathematically expressed as follows:

$$W(f_1, f_2) = \frac{H^*(f_1,f_2) S_{xx}(f_1,f_2)}{|H(f_1,f_2)|^2 S_{xx}(f_1,f_2) + S_{\tau\tau}(f_1,f_2)'} \quad (9)$$

where, $S_{xx}(f_1, f_2)$ is the power spectral of the original image, $S\tau\tau(f_1, f_2)$ is the power spectral of additive Gaussian noise, $H(f_1, f_2)$is the blurring filter (Vaseghi, 2001).

I) Equalization

Histogram Equalization is an image processing technique used to improve image contrast. It achieves this by effectively spreading out the most common intensity values of pixels across the screen, stretching out the intensity range.

J) Weighted Average

Over-enhancement is a common issue with image filtering. Here, a weighted average is applied to the filtered and equalised images to reduce the excessive enhancement.

A= $\sum_1^3$ filtered (IMFi)

N= A.* Q + β *B.* (unit matrix - Q) (10)

where;.* represents the bit wise multiplication. β is the brightness compensation factor(1<β< 2). Q and (unit matrix – Q) are the weighting coefficients of A and B (Lidong et al, 2015).

$$Q=\begin{bmatrix} Q(1,1) & \cdots & Q(1,n) \\ \vdots & \ddots & \vdots \\ Q(m,1) & \cdots & Q(m,n) \end{bmatrix} = \begin{bmatrix} f(A(1,1))^{\gamma} & \cdots & f(A(1,q))^{\gamma} \\ \vdots & \ddots & \vdots \\ f(A(p,1))^{\gamma} & \cdots & f(A(\mathrm{p},\mathrm{q}))^{\gamma} \end{bmatrix} \quad (11)$$

Both A and B have the same size, p × q. For optimal brightness preservation the range of γ is fixed between [0, 5] and for this observation, γ is set to 1.5.The maximum and minimum grey values of image A are represented by max(A) and min(A). The function used in Eq. (11) is described as:

$$f(\mathrm{A}(\mathrm{i},\mathrm{j})) = \frac{A(i,j)-\min(A)}{\max(A)-\min(A)} \quad (12)$$

III. RESULTS AND DISCUSSION

The performance of the proposed method is evaluated subjectively using performance metrics such as Mean Square Error (MSE), Peak Signal to Noise Ratio (PSNR), Structural Similarity Index Measure (SSIM), Absolute Average Difference(AAD), Maximum Difference (MD), Mean Absolute Error (MAE), Normalize Absolute Error (NAE), pearson correlation coefficient (CORR), Normalized Cross Correlation (NCC) and Structural Content (SC).In this paper, a set of standard MRI brain images with a 256x256 size was investigated. For this study, Matlab 14a with an Intel (R) 2.40 GHz CPU and 4 GB of memory was used. During the experiment, the original image is added with noise (salt and pepper noise, Gaussian noise, speckle noise) having different variances. The noisy images with a variance of 0.01 are shown in Figs. 4-6. The proposed denoising technique is compared with three state-of-the-art filtering methods like the Median Filter, Gaussian Filter, and Wiener Filter. The comparative results are demonstrated in Figs. 7-9.

A) Metrics of Performance Measures

1) Root mean square error

The MSE represents the aggregate of the square of the error between the de-noised image and the reference image. The lower the value of MSE indicates the closeness of the two images used for comparison purposes. The Eqn. (9) is used for MSE calculation.

$$\mathrm{MSE} = \frac{1}{pq}\sum_{a=0}^{p-1}\sum_{b=0}^{q-1}[M(a,b)-N(a,b)]^2 \quad (13)$$

where, *p q*: Dimension of the image.

M (a, b): Intensity of pixels (a, b) original image.

N(a,b):Intensityof pixels (a, b) after de-noising.

RMSE = $\sqrt{\mathrm{MSE}}$

2) Peak signal-to-noise ratio

The peak signal-to-noise ratio (PSNR) is the ratio of the signal power of the processed image to the referral image. The Higher value of PSNR represents a better quality of performance. PSNR is represented as:

$$PSNR_{db} = 10log_{10}(\frac{MAX^2}{MSE}) \quad (14)$$
$$=20log_{10}(\mathrm{MAX}) - 10log_{10}(MSE)$$

MAX is the maximum possible pixel value of the original image which is 255 in 8-bit image systems.

3) Structural similarity index

The SSIM is a perceptual metric used for quantifying the image quality which was degraded by the process of data compression, data transmission, and data acquisition. It is a full reference metric comparison method that requires a minimum of two images as the reference image and a processed image. The range of the SSIM is between -1 to1 to indicate the similarity. The closer to the value of 1 is more similar in structure.

$$\mathrm{SSIM}(\mathrm{M},\mathrm{N}) = [\mathrm{q}(\mathrm{M},\mathrm{N})]^{\alpha}[\mathrm{w}(\mathrm{M},\mathrm{N})]^{\beta}\ [\mathrm{e}\ (\mathrm{M},\mathrm{N})]^{\gamma} \quad (15)$$

where,

$$q(M,N) = \frac{2\mu_M\mu_N+C_1}{\mu_M^2+\mu_N^2+C_1} \quad (16)$$

$$W(M,N) = \frac{2\delta_M\delta_N+C_2}{\delta_M^2+\delta_N^2+C_2} \quad (17)$$

$$e(M,N) = \frac{\delta_{MN}+C_3}{\delta_M\delta_N+C_3} \quad (18)$$

where,

$\mu_M = Localmeanforiamgea$

$\mu_N = localmeanforimageb$

$\delta_M = standraddeviationforimagea$

δ_{MN}= cross co-variance for image a,b

$\delta_N = standraddeviationforimage$b

If α = β = γ = 1 and C_3= C_2/2 then the above index is simplifying to:

$$SSIM = \frac{(2\mu_M\mu_N+C_1)(2\delta_M\delta_N+C_2)}{(\mu_M{}^2+\mu_N{}^2+C_1)(\delta_M{}^2+\delta_N{}^2+C_2)} \quad (19)$$

4) Absolute Average Difference (AAD)

The absolute average difference provides the average amount of change between the processed and reference image (Jagalingam and Hegde, 2015). AAD can be expressed as follows:

$$AAD = \left|\frac{1}{\mathrm{pq}}\sum_{\mathrm{a}=0}^{\mathrm{P}-1}\sum_{\mathrm{b}=0}^{\mathrm{q}-1}[\mathrm{M}(\mathrm{a},\mathrm{b})-\mathrm{N}(\mathrm{a},\mathrm{b})]\right| \quad (20)$$

5) Maximum Difference (MD)

The maximum value of the absolute error between the processed and reference image is one of the important factor in quality assessment and is represented as follows:

$$MD = \mathrm{Max}\ (|M\ (a,b)-N(a,b)|) \quad (21)$$

6) Mean Absolute Error (MAE)

MAE is defined as the maximum absolute value, the difference between the original image and the reconstructed image (Naidu and Raol 2008). As the name suggests, the mean

absolute error is an average of the absolute errors. MAE values range from 0 to 255, and the lower MAE value, the better demosaicing quality.

$$MAE = \frac{\sum_{a=0}^{p-1}\sum_{b=0}^{q-1}(|X(a,b)-Y(a,b)|)}{p\times q} \quad (22)$$

7) Normalize Absolute Error (NAE)

This quality measure can be expressed as follows:

$$NAE = \frac{\sum_{a=0}^{p-1}\sum_{b=0}^{q-1}(|X(a,b)-Y(a,b)|)}{\sum_{a=0}^{P-1}\sum_{b=0}^{q-1}X(i,j)} \quad (23)$$

A higher *NAE* value shows that image is of poor quality.

8) Correlation (CORR)

The Pearson correlation coefficient computes the similarity features of the reference image and fused image. The benchmark correlation value is one when the fused and reference are exactly alike. A higher value of SC (Structural Content) shows that image is of poor quality.

9) Normalized Cross Correlation (NCC)

NCC (Normalized Cross Correlation) measure shows the comparison of the processed image and reference image (Tiwari and Singh 2004). NCC is expressed as follows:

$$NCC = \sum_{a=0}^{P-1}\sum_{b=0}^{q-1}\frac{(M(a,b)\times N(a,b))}{M(a,b)^2} \quad (24)$$

Furthermore, the Normalized Cross Correlation is confined in the range between –1 and 1 (Tiwari and Singh, 2004). NCC is expressed as follows:

10) Structural Content (SC)

This quality metric is expressed as follows:

$$SC = \frac{\sum_{a=0}^{p-1}\sum_{b=0}^{q-1}M(a,b)^2}{\sum_{a=0}^{P-1}\sum_{b=0}^{q-1}N(a,b)^2} \quad (25)$$

B) Performance Analysis

In this section, the suggested model is tested according to the method discussed in Section II. For this experiment, a set of grey-level brain MRI images of 256x256 pixels is considered (Hamada 2020). The results are validated using a four-level empirical mode decomposition technique. Each test was repeated with ten different measuring parameters, and the average value of each performance measure is shown in Tables 1 through 3. The range of noise variance examined in each experiment is 0.001 to 0.1.

A few examples of MRI brain images are shown in Figures 7 to 9 for objective analysis of the proposed method. In figure 7, we have considered salt and pepper noise. Figure 7 (b) represents a noisy image with noise density 0.01. The sub Figure 7(c), 7(d) and 7(e) are showing the results of median, wiener and Gaussian filter processed image. These results are evidence that these filters are not only filtering the noise but also capable of preserving brightness. But when the Gaussian filter is considered with BEMD, the contrast of the image is also improved and the image is objectively looks better.

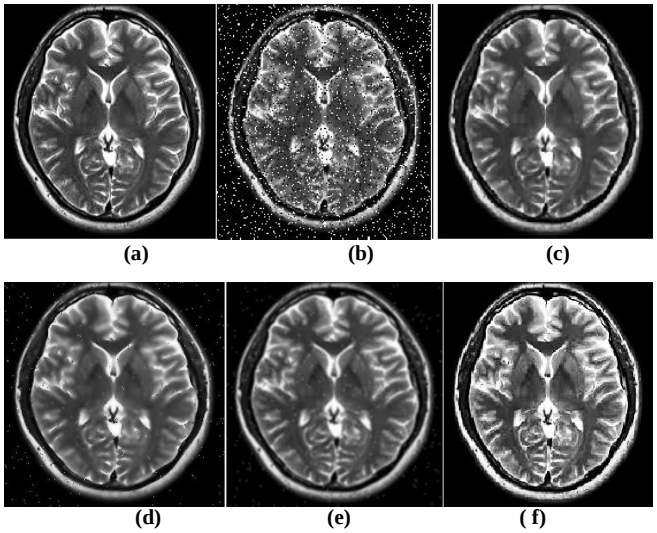

Figure 7: (a) Input MRI brain image (b) Image with Salt and pepper noise with density 0.1 (c) median filtered image (d)wiener filtered image(e) Applying Gaussian filtered image (f) Proposed BEMD with Gaussian filter method.

Similar experiments were conducted for Gaussian noise and Speckle noise, and the evidence were recorded in Figures 8 and 9. In each case BEMD with Gaussian filtered images are looks better as compared to median filter, wiener filter and Gaussian filter processed image.

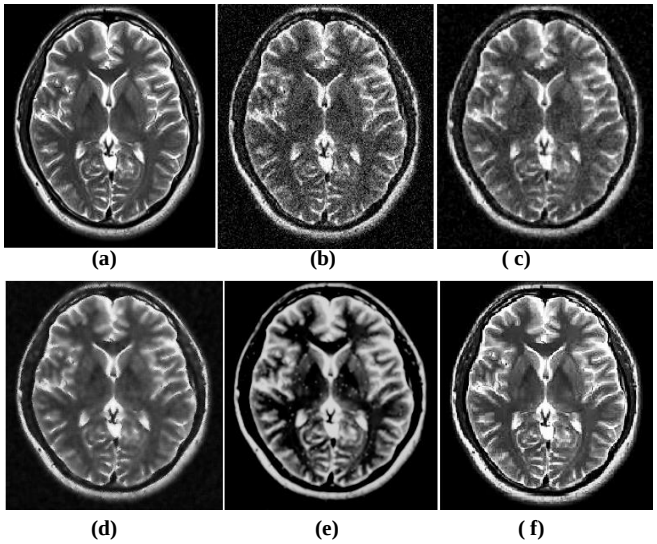

Figure 8 (a) Input image (b) Image with Gaussian noise and variance 0.01 (c) median filtered image (d) wiener filtered image (e) Applying Gaussian filtered image (f) Proposed BEMD with Gaussian filter method with Gaussian filter method.

The proposed method describes the hybridization of classic filters with BEMD. To quantify the method a number of different gray images are considered (Chakrabarty, 2018) and the average value of PSNR, MSE and SSIM are calculated. The bar chart result of each of the above mentioned metrics are represented in Figures 10 to 12.

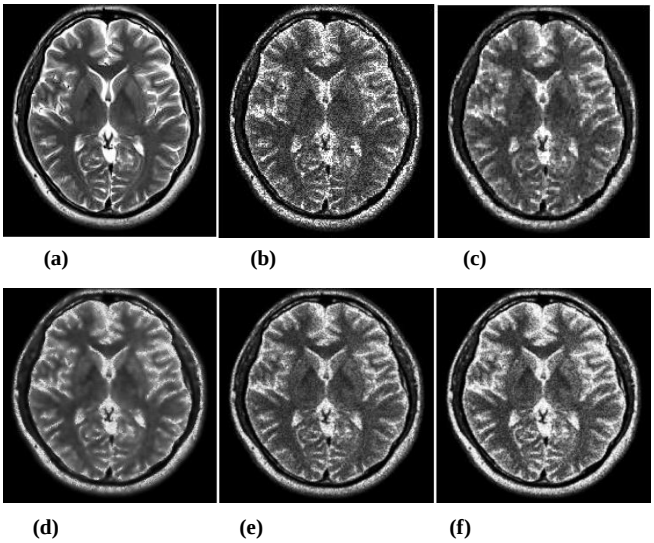

Figure 9: (a) Input MRI brain image (b) Image with Speckle noise with variance 0.1) (c) Median filtered image (d) wiener filtered image(e) Applying Gaussian filtered image (f) Proposed BEMD with Gaussian filter method.

Figure 10 provides a comparative analysis of PSNR values in a bar chart. For a variance of 0.001, the graph shows that the bemd based filtering methods has a higher PSNR value than the median, Gaussian and wiener filter. As per literature the higher PSNR is the evidence of better noise reduction. Similarly the effectiveness of the method interms of MSE and SSIM can be seen in Fig. 11 and 12 respectively. Increasing SSIM and decreasing MSE validates the proposed method's effectiveness. The higher the SSIM value, the more likely the structure will be retained.

The average value of RMSE, PSNR, and SSIM for a set of images is calculated, and all results are listed in Table I-III. Table I depicts the result of the images being affected by Gaussian noise. It was observed that when bemd-based filtering was compared to direct filtering, the PSNR values increased. The higher value of SSIM indicates the structural closeness between the original and the processed image in the proposed method. The lower value of RMSE is an indicator of brightness preservation. Table 1 also shows some of the error metrics, including absolute average difference,

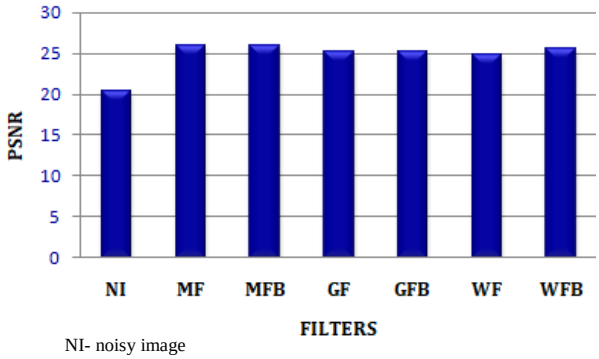

NI- noisy image
MF-median filter
GF- Gaussian filter
WF- wiener Filter
MBF- median filter with BEMD
GFB- Gaussian filter with BEMD
WFB- wiener filter with BEMD

Figure 10: Comparison of PSNR value for Gaussian noise affected image filtered by different methods and the proposed method.

maximum difference, mean absolute error, normalised absolute error and structural content. The lower the value of the metrics, the more effective the method is. The greater Pearson correlation coefficient and normalised cross correlation value indicate that the two images have a very strong, significant, and positive relationship.

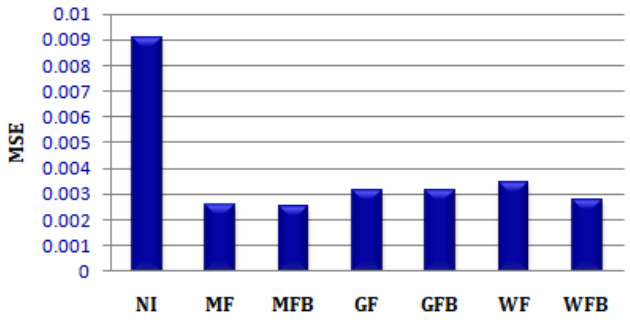

NI- noisy image
MF-median filter
GF- Gaussian filter
WF- wiener Filter
MBF- median filter with BEMD
GFB- Gaussian filter with BEMD
WFB- wiener filter with BEMD

Figure 11: Comparison of MSE value for Gaussian noise affected image filtered by different methods and the proposed method.

Similarly in Tables 2 and 3, metrics were calculated using speckle noise and salt and pepper noise. It was observed from the tables that in the presence of speckle noise and salt and pepper noise, the Gaussian filter and BEMD with Gaussian filter have nearly same PSNR value. However, in the case of salt pepper noise in Table 3, it was discovered that the median filter's PSNR value is higher than BEMD with median filter, which contradicts the effectiveness of the method. According to Wang and Bovik, the MSE and PSNR can yield contradictory findings in some circumstances, even if the outcome appears to be visually pleasing (Wang and Bovik, 2009). As per the findings presented in Tables 1 to 3, the median filter likewise outperforms the others for all noises.

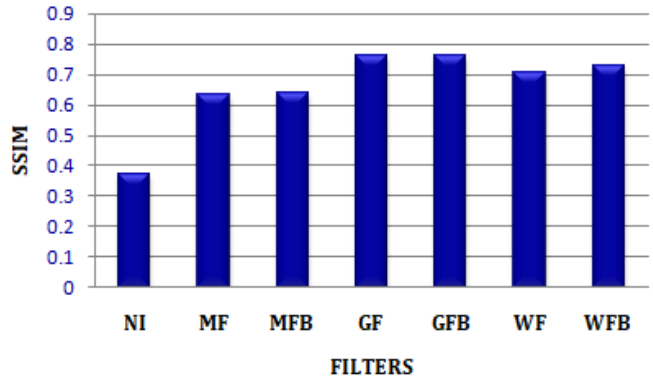

NI- noisy image
MF-median filter
GF- Gaussian filter
WF- wiener Filter
MBF- median filter with BEMD
GFB- Gaussian filter with BEMD
WFB- wiener filter with BEMD

Figure 12: Comparison of SSIM value for Gaussian noise affected image filtered by different methods and the proposed method.

IV. CONCLUSION

In this study, we have proposed a new method of algorithm for image denoising. The objective of this method is to exploit the advantages of empirical mode decomposition with a multi-resolution structure and also to demonstrate the model's resemblance to the human visual system as well as its remarkable spatial and frequency localization features. In this technique, the first IMF does not contain all the noise, so the standard filter is applied to all IMFs except the residuals. The suggested method was tested on a set of images contaminated by different types of noise. Experiments on benchmark images demonstrate that the proposed technique outperforms similar types of denoising algorithms, particularly in terms of PSNR, MSE, SSIM index, and visual effect. The obtained results do not suffer from over smoothing and loss of details. Future research will look into a soft computing-based threshold factor, which will be applied to the coefficients of the decomposed image to improve the denoising performance.

CONFLICT OF INTERESTS

The authors declare that they have no conflict of interests.

AVAILABILITY OF DATA AND MATERIALS

The datasets used and/or analyzed during the current study are available from the corresponding author on request.

AUTHOR CONTRIBUTIONS

Both authors contributed equally in this work. The authors read and approved the final manuscript.

FUNDING SOURCE

There is no source of funding for the research.

.

Table 1. Comparison of PSNR, MSE, SSIM of different filters concerning the proposed method for Gaussian noise affected image.

	PSNR	RMSE	SSIM	AAD	MD	MAE	NAE	CORR	NCC	SC
Noisy Image	20.46	0.0952	0.3693	3.7514	91	6.3035	0.3239	0.9190	0.9159	0.91
Median Filter	25.93	0.0507	0.6346	0.6985	101	4.5187	0.1920	0.9662	1.0033	1.04
Gaussian Filter	25.13	0.0563	0.7634	3.7330	74	3.9944	0.2310	0.9598	0.9698	0.98
Wiener Filter	24.74	0.0586	0.7080	3.8644	87	3.3549	0.2087	0.9724	0.9983	1.03
Proposed method with Median Filter	25.97	0.0503	0.6370	0.5871	92	3.9255	0.1511	0.9786	1.0007	1.02
Proposed method with Gaussian Filter	25.16	0.0561	0.7635	2.9750	71	3.2714	0.2022	0.9692	0.9792	0.99
Proposed method with Wiener Filter	25.62	0.0529	0.7288	3.2131	82	2.9918	0.1977	0.9815	0.9988	1.02

Table 2: Comparison of PSNR, MSE, SSIM of different filters with respect to the proposed method for Speckle noise affected image.

	PSNR	RMSE	SSIM	AAD	MD	MAE	NAE	CORR	NCC	SC
Noisy Image	20.46	0.0952	0.3693	2.0629	88	8.85	0.1924	0.9569	0.9556	0.9635
Median Filter	21.61	0.0839	0.5184	1.6906	118	4.42	0.1462	0.9718	1.0322	1.1073
Gaussian Filter	23.63	0.0693	0.7426	0.0718	84	3.41	0.1345	0.9779	0.9941	1.0185
Wiener Filter	23.00	0.0744	0.6599	0.2496	117	3.68	0.1510	0.9725	1.0025	1.0409
Proposed method with Median Filter	21.76	0.0825	0.5251	1.6301	109	4.11	0.1377	0.9811	1.0122	1.0722
Proposed method with Gaussian Filter	23.66	0.0690	0.7437	0.0677	81	3.19	0.1224	0.9856	0.9961	1.0082
Proposed method with Wiener Filter	23.60	0.0693	0.6750	0.2288	112	3.37	0.1421	0.9837	1.0015	1.0235

Table 3. Comparison of PSNR, MSE, SSIM of different filters with respect to the proposed method for Salt and Peeper noise affected image.

	PSNR	RMSE	SSIM	AAD	MD	MAE	NAE	CORR	NCC	SC
Noisy Image	20.46	0.0952	0.3693	3.7896	231	1.2506	0.1283	0.82	0.82	0.8042
Median Filter	30.27	0.0436	0.7310	0.5225	143	1.8731	0.0841	0.98	0.98	1.0539
Gaussian Filter	23.55	0.0676	0.6818	3.7795	171	5.9569	0.1582	0.90	0.92	0.9207
Wiener Filter	22.48	0.0759	0.6101	3.7424	195	7.5926	0.2230	0.91	0.96	0.9967
Proposed method with Median Filter	27.53	0.0428	0.7403	0.5117	128	1.5722	0.0819	0.99	0.99	1.0321
Proposed method with Gaussian Filter	23.57	0.0671	0.6820	3.7318	159	5.1176	0.1477	0.93	0.93	0.9427
Proposed method with Wiener Filter	22.82	0.0728	0.6147	3.7338	172	7.2426	0.2112	0.94	0.97	0.9972

REFERENCES

Adamo, F.; Andria, G.; F. Attivissimo; A. M. L. Lanzolla, and M. Spadavecchia (2013). Acomparative study on mother wavelet selection in ultrasound image denoising. Measurement,46(8):2447–2456.

Bnou, K.; S. Raghay and A. Hakim (2020). A wavelet denoising approach based on unsupervised learning model. EURASIP J. Adv. Signal Process.36.

Chang, S. G.; B. Yu and M. Vetterli (2000). Adaptive wavelet thresholding for image denoising and compression, in IEEE Transactions on Image Processing, 9(9):1532-1546.

Dong, W.; X. Li; X. Lin and Z. Li (2014). A Bidimensional Empirical Mode Decomposition Method for Fusion of Multispectral and Panchromatic Remote Sensing Images. Remote Sensing.6:8446-8467.

Donoho, D. L.(1995). De-noising by soft-thresholding, in IEEE Transactions on Information Theory, 41(3) : 613-627.

Ellinas, J. N.; T. Mandadelis,; A. Tzortzis, and L. Aslanoglou, (2004). Image de-noising using wavelets. TEI of Piraeus Applied Research Review, 9(1), 97-109.

Fedak, V. and Nakonechnyy, A. (2015). Adaptive wavelet thresholding for image denoising using SURE Minimizationand Clustering of Wavelet Coefficients. Technical Transaction on Electrical Engineering, 197–210.

Gonzalez, R. C. and Woods, R. E. **(2007).** Digital Image Processing. Englewood Cliffs, NJ:Prentice-Hall.

Gupta, D. and Ahmad, M. (2018). Brain MR image denoising based on wavelet transform. Int. J. Appl. Technol. Eng. Explor, **5**(38): 11–16.

Hamada A. (2020), Brain tumor detection, Available online at: https://www.kaggle.com/navoneel/brain-mri-images-for-brain-tumor-detection (collected on 15/03/2021)

Huang, N. E.; Shen, Z.; Long, S. R.; Wu, M. C.;Shih, H. H.; Zheng, Q. ; Yen, N. ; Tung, C. C. , and Liu, H. H. (1998). The empirical mode decomposition and the Hilbert spectrum for nonlinear and non-stationary time series analysis Proc. R. Soc. Lond. A.454903–995

Kimlyk, M., and Umnyashkin, S. (2018). Image denoising using discrete wavelet transform and edge information. IEEE Conference of Russian Young Researchers in Electrical and Electronic Engineering (EIConRus): 1823-1825.

Kumar, B. K. S. (2013). Image denoising based on non-local means filter and its method noise thresholding. Signal, Image and Video Processing,7(6):1211–1227.

Lidong, H.; Wei, Z.; Jun, W., and Zebin, S. (2015). Combination of contrast limited adaptive histogram equalisation and discrete wavelet transform for image enhancement, IET Image Process, 9(10): 908-915.

Madadi, Z.; G. V. Anand and A.B. Premkumar (2013). Signal detection in generalized Gaussian noise by nonlinear wavelet denoising. IEEE Trans. Circuits Syst. I Reg. Papers, 60(11) :2973-2986.

Mallat, S. (2008). A Wavelet tour of signal processing: the sparse way, 3rd edition. Academic Press, Elsevier, Burlington.

Naidu, V. P. S. and Raol, J. R. (2008). Pixel-level image fusion using wavelets and principal component analysis. Defense ScienceJournal. 58(3):338–52.

Qi, C., and Li, Q. (2016). The improved method of wavelet denoising for nonlinear signal, Manufacturing Automation, 38:14-17.

Sagheer, S. V. M. and George, S. N. (2020). A review on medical image denoising algorithms, Biomedical Signal Processing and Control,Vol. 61.

Satapathy, L. M.; A. Dalai; S. Satapathy and A. Jena (2018). Satellite image enhancement based on multi-technology fusion, 2018 Second International Conference on Inventive Communication and Computational Technologies (ICICCT), Coimbatore, 1677-1680.

Srivastava, M.; C. L. Anderson, and J. H. Freed (2016). A new wavelet denoising method for selecting decomposition levels and noise thresholds, IEEE Access Practical Innovations Open Solutions, 4: 3862-3877.

Tiwari, A., and Singh, P. (2014). Analysis of Color Contrast Enhancement Techniques, International Journal of Emerging Technology and Advanced Engineering,4(4):185-191

Yan, R.; L. Shao and Y. Liu, (2013). Nonlocal hierarchical dictionary learning using wavelets for image denoising. IEEE Transactions on Image Processing, 22(12):4689–4698

Zhang, X. (2016). Image denoising using dual-tree complex wavelet transform and wiener filter with modified thresholding. J Sci Ind Res India, 75(11):687–690.

Zhou W. and Bovik, A. (2009). Mean squared error: Love it or leave it? A new look at Signal Fidelity Measures, in IEEE Signal Processing Magazine, 26(1): 98-117.